Pergamon

Computers and Chemical Engineering Supplement (1999) S241–S244
© 1999 Elsevier Science Ltd. All rights reserved
PII: S0098-1354/99/00222-7

Nonlinear Control of Rapid Thermal Chemical Vapor Deposition Under Uncertainty

James Baker and Panagiotis D. Christofides

Department of Chemical Engineering, University of California, Los Angeles, CA 90095-1592, USA

Abstract. This article focuses on nonlinear control of a rapid thermal chemical vapor deposition (RTCVD) process in the presence of significant model uncertainty and disturbances. Initially, a detailed mathematical model of the RTCVD process is presented consisting of a nonlinear parabolic partial differential equation (PDE) which describes the time evolution of the wafer temperature across the radius of the wafer, coupled with a set of nonlinear ordinary differential equations (ODEs), which describe the time evolution of the concentrations of the various species. Then, the synthesis of a nonlinear output feedback controller based on the RTCVD process model by following a control methodology for nonlinear parabolic PDE systems introduced in (Baker and Christofides, 1998) is discussed. The controller uses measurements of wafer temperature at four locations to manipulate the power of the top lamps in order to achieve uniform temperature, and thus, uniform deposition of the thin film on the wafer over the entire process cycle. The nonlinear output feedback controller is successfully implemented through computer simulations and is shown to attenuate significant model uncertainty and disturbances and to outperform a proportional integral (PI) control scheme.

Key Words. Parabolic PDE systems, Nonlinear model reduction, Nonlinear output feedback control, Rapid thermal processing

1. Introduction

Rapid thermal chemical vapor deposition (RTCVD) is a rapidly growing technology in the microelectronics industry. The central idea of RTCVD is to use a series of lamps to radiatively heat a thin silicon wafer from room temperature to 1200 K at very high heating rates (more than 150 K/s), and then keep it at the high temperature for a short time. This sharp increase in the temperature of the wafer reduces significantly the overall thermal budget of the process (the overall processing time is usually less than a minute) and the diffusion length, thereby preserving dopant profiles from previous steps, and allows the fabrication of very small devices by using temperature as a switch in ending a process cycle. These features make RTCVD an attractive alternative over conventional furnace-based chemical vapor deposition processes employed in the fabrication of devices with submicron dimensional constraints. Even though RTCVD possesses many significant advantages, its widespread use is seriously limited by the lack of adequate wafer temperature control to achieve the tight requirements of uniformity and repeatability set by the industry. The main obstacles in achieving spatially uniform wafer temperature (and thus, uniform film deposition) are the highly nonlinear (owing to the radiative heat transfer mechanism), dynamic (owing to the very rapid heating of the wafer) and spatially varying nature of the RTCVD process that makes the development and implementation of effective model-based feedback controllers a very difficult task (see, for example, (Breedijk *et al.*, 1993; Schaper, 1993; Stuber *et al.*, 1995; Butler and Edgar, 1997; Kiether *et al.*, 1994; Theodoropoulou *et al.*, 1998*a*) for previous results on control). The main challenge in the design of model-based feedback controllers for RTCVD processes is that the dynamic models of such processes consist of nonlinear parabolic partial differential equation (PDE) systems, which are distributed parameter (infinite-dimensional) systems, and thus, they cannot be directly used for the design of practically implementable (low-dimensional) controllers (Aling *et al.*, 1997).

This article focuses on nonlinear control of an RTCVD process in the presence of significant model uncertainty and disturbances. Initially, a detailed mathematical model of the RTCVD process is presented which consists of a nonlinear parabolic PDE which describes the time evolution of the wafer temperature across the radius of the wafer, coupled with a set of nonlinear ODEs, which describe the time evolution of the concentrations of the various species. Then, the synthesis of a nonlinear output feedback controller based on the RTCVD process model by following a control methodology for nonlinear parabolic PDE systems introduced in (Baker and Christofides, 1998) is discussed. The controller design method consists of three steps: first, the Karhunen-Loeve decomposition is used to derive empirical eigenfunctions of the nonlinear parabolic PDE system, then the empirical eigenfunctions are used as basis functions within a Galerkin's model reduction framework to derive low-order ODE systems that accurately describe the dominant dynamics of the PDE system, and finally, these ODE systems are used for the synthesis of nonlinear output feedback controllers that guarantee stability and enforce output tracking in the closed-loop system. The controller uses measurements of wafer temperature at four locations to manipulate the power of the top lamps in order to achieve uniform temperature, and thus, uniform deposition of the thin film on the wafer over the entire process cycle. The

Financial support for this work from NSF, Grant CTS-9733509, is gratefully acknowledged.

ability of the nonlinear output feedback controller in achieving a spatially uniform temperature profile (and therefore, final film thickness) in the presence of significant model uncertainty and disturbances is successfully tested through simulations and is shown to be superior to that of a PI control scheme.

2. RTCVD Description and Modeling

We consider a low pressure rapid thermal chemical vapor deposition (RTCVD) process shown in Figure 1. This process closely resembles an experimental

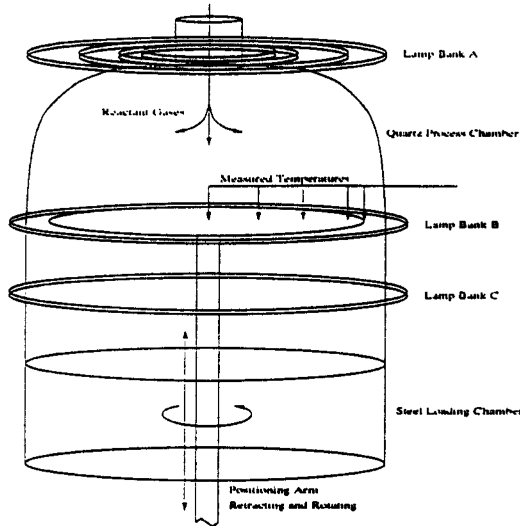

Fig. 1. Rapid thermal chemical vapor deposition.

RTCVD reactor located at the North Carolina State University Center for Advanced Electronic Materials Processing (Kiether *et al.*, 1994) (see also (Theodoropoulou *et al.*, 1998*b*)). The process consists of a quartz chamber, three banks of tungsten heating lamps which are used to heat the wafer and a fan which is located at the bottom of the reactor and is used to cool the chamber. The furnace is designed so that the top lamp bank A and the bottom lamp bank C heat the total area of the wafer, while the lamp bank B, which surrounds the reactor, is used to heat the wafer edge in order to compensate for heat loss that occurs from the edge (radiative cooling between wafer edge and quartz chamber). The wafer is rotated while heated for azimuthal temperature uniformity. A small opening exists on the top of the quartz chamber which is used to feed the reacting gases. The objective of the process is to deposit a $0.51\mu m$ film of polycrystalline silicon on a 6-inch wafer in 40 seconds. To achieve this objective, the reactor is fed with 10% SiH_4 in Ar at 5 $Torr$ pressure and the heating lamps are used to heat the wafer from room temperature to $1200K$ (this is the temperature where the deposition reactions take place), at a heating rate of the order of $180K/sec$.

A detailed mathematical model for the RTCVD process has been developed in (Theodoropoulou *et al.*, 1998*b*) under the following standard assumptions (see also (Breedijk *et al.*, 1993) for similar assumptions):

1. Wafer temperature uniformity in the azimuthal direction due to wafer rotation and symmetric reactor design.
2. Negligible wafer temperature variations in the axial direction due to small thickness of the wafer.
3. Negligible heat transfer from the wafer to the reactant gases due to low pressure conditions inside the chamber.
4. Negligible heat of deposition reactions compared to radiative heat transfer from the lamps to the wafer.
5. Constant optical properties of the wafer and the chamber.
6. Perfect mixing of the reacting mixture.
7. Spatially uniform quartz chamber wall thermal dynamics.

Under the above assumptions, an energy balance on the wafer yields the following nonlinear parabolic PDE:

$$\rho_w T_{amb}\frac{\partial}{\partial t}\left(C_{p_w}(T)T\right) = \frac{T_{amb}}{R_w^2}\frac{1}{r}\frac{\partial}{\partial r}\left(\kappa(T)r\frac{\partial T}{\partial r}\right) - \frac{q_{rad}(T,r)}{\delta z} \tag{1}$$

subject to the boundary conditions

$$\left.\frac{\partial T}{\partial r}\right|_{r=0} = 0 \tag{2}$$

$$\left.\frac{T_{amb}}{R_w}\kappa(T)\frac{\partial T}{\partial r}\right|_{r=1} = -\sigma\epsilon_w T_{amb}^4(T^4 - T_c^4) + q_{edge}u_b \tag{3}$$

In the above equations, T_{amb} denotes the ambient temperature, $T = \frac{T'}{T_{amb}}$ denotes the dimensionless wafer temperature, ρ_w, C_{p_w}, R_w denote the density, heat capacity and radius of the wafer, $r = \frac{r'}{R_w}$ denotes the dimensionless radial coordinate, q_{rad} is a term that accounts for radiative energy transfer between the wafer and its environment (see below for an explicit statement of the radiative phenomena contributing to this term), $T_c = \frac{T_c'}{T_{amb}}$ denotes the dimensionless temperature of the chamber, σ denotes the Stefan-Boltzmann constant, ϵ_w denotes the emissivity of the wafer, q_{edge} denotes the energy flux at the edge of the wafer, u_b denotes the percentage of the side lamp power that is used. The wafer heat capacity and thermal conductivity depend on temperature according to the following relations:

$$\begin{aligned}\kappa(T) &= 50.5ln(TT_{amb})^2 - 734.0ln(TT_{amb}) \\ &\quad +2.69\times 10^3\ W/m\ K \\ C_{p_w}(T) &= 1.06\times 10^3 - 1.04\times 10^5/(TT_{amb})\ J/(Kg\ K)\end{aligned} \tag{4}$$

The radiative energy transfer term q_{rad} consists of two parts: the radiant energy absorbed from the heating lamps and the radiant energy exchanged between the wafer and reactor walls i.e.:

$$q_{rad} = -Q_{lamps,w}\cdot u + q_{dw,t} + q_{dw,b} \tag{5}$$

where $Q_{lamps,w}$ is a vector of the total energy emitted

from the three lamp banks and absorbed by the wafer, $u = [u_A u_B u_C]$ is the percentage of the lamp power that is used, $q_{dw,t}$ ($q_{dw,b}$) is the net radiative energy transfered to the wafer top (bottom) surface from sources other than the lamps (e.g., reflection from the quartz process chamber). The heating lamp energy flux to the wafer surface, $Q_{lamps,w}$, is computed by a ray-trace algorithm, which calculates the radiant energy flux distributions directly from the lamps to the wafer as well as the contribution of the reflected rays. The radiant energy flux distribution for each lamp bank as a function of wafer radial position can be found in (Theodoropoulou *et al.*, 1998*b*). The radiation exchange between the wafer and the walls (terms $q_{dw,t}$ and $q_{dw,b}$) is computed using the net-radiation method. We note that $q_{dw,t}, q_{dw,b}$ are highly nonlinear functions of the wafer and chamber temperatures, geometry of the reactor and emissivity of wafer and chamber.

An energy balance on the quartz chamber yields the following ordinary differential equation.

$$T_{amb} M_c \frac{dT_c}{dt} = \epsilon_c Q_{lamps} \cdot u - A_{hem}\, q_h - A_{cyl}\, q_c - Q_{convect} - \sigma \epsilon_c A_c T_{amb}^4 (T_c^4 - 1) \qquad (6)$$

where M_c denotes the chamber thermal mass, ϵ_c denotes the emissivity of the chamber, A_{hem} denotes the chamber hemispherical area, A_{cyl} denotes the chamber cylindrical area and A_c denotes the chamber outside area. q_h and q_c denote the net energy radiated from the hemispherical and cylindrical portions of the quartz chamber, respectively, and their expressions computed from the net-radiation method can be found in (Theodoropoulou *et al.*, 1998*b*). The term $Q_{lamps} \cdot u$ represents energy absorbed by the chamber directly from the heating lamps, while $Q_{convect}$ denotes the energy transfered from the quartz chamber to the cooling gas by forced convective cooling. The explicit computation of $Q_{convect}$ can be done by a simple cooling gas energy balance and is given in (Theodoropoulou *et al.*, 1998*b*).

The assumption of perfect mixing of the reacting mixture allows us to derive the following set of ODEs which describe the time evolution of the molar fraction of SiH_4, X_{SiH_4}, and hydrogen, X_{H_2}:

$$\begin{aligned} \frac{dX_{SiH_4}}{dt} &= -\alpha \int_{A_w} R_s(T, X_{SiH4}, X_{H2})\, dA_w + \frac{1}{\tau}(X_{SiH_4}^{in} - X_{SiH_4}) \\ \frac{dX_{H_2}}{dt} &= 2\alpha \int_{A_w} R_s(T, X_{SiH4}, X_{H2})\, dA_w - \tfrac{1}{\tau} X'_{H_2} \end{aligned} \qquad (7)$$

where α is the mole to mole conversion factor, A_w is the wafer area, τ is the residence time, $X_{SiH_4}^{in}$ is the molar fraction of SiH_4 in the inlet stream to the reactor and R_s is the rate of the deposition reactions:

$$R_s(T, X_{SiH4}, X_{H2}) = \frac{k_0\, exp\left(\dfrac{-\gamma}{R\,T\,T_{amb}}\right) X_{SiH_4} P_{tot}}{1 + b X_{SiH_4} P_{tot} + \dfrac{\sqrt{X_{H_2} P_{tot}}}{c}} \qquad (8)$$

where k_0 is the pre-exponential constant, γ is the activation energy for deposition, P_{tot} is the total pressure and b, c are constants. The deposition rate of Si onto the wafer surface is governed by the following expression:

$$\frac{dS}{dt} = \frac{MW_{Si}}{\rho_{Si}} R_s(T, X_{SiH_4}, X_{H_2}) \qquad (9)$$

where MW_{Si} and ρ_{Si} denote the molecular weight and density of Si, respectively. Referring to the expression of the deposition rate, we note the Arrhenius dependence of the deposition rate on wafer temperature which clearly shows that nonuniform temperature results in nonuniform deposition, thereby implying the need to develop and implement a nonlinear feedback controller on the process in order to achieve radially uniform wafer temperature.

3. Controller Design - Closed-loop Simulations

The objective of this section is to test the robustness properties of a nonlinear low-order output feedback controller synthesized in (Baker and Christofides, 1998) for the RTCVD process in the presence of significant model uncertainty and disturbances. A brief description of the procedure followed for the synthesis of the controller is given below (all the details can be found in (Baker and Christofides, 1998)). A second-order finite difference scheme with 100 discretization points was initially used to compute an accurate solution of the model of the RTCVD process (Eqs.1-6-7). For time integration, the Euler method was used. Following (Theodoropoulou *et al.*, 1998*b*), the nonlinear boundary condition of Eq.3 was solved simultaneously at each time step using a Gauss-Newton method. Several 40 second simulation runs of the process were performed with the following initial conditions: $T = 1$, $T_c = 1$, $S = 0$, $X_{SiH_4} = 0.1$ and $X_{H_2} = 0$. "Snapshots" of the temperature profiles were used as data for determining the dominant spatial temperature modes (wafer temperature empirical eigenfunctions) through Karhunen-Loéve decomposition. Then, a collocation formulation of Galerkin's method was used to obtain a low-order model that describes the wafer temperature. The wafer temperature was expanded in terms of the first four empirical eigenfunctions. The three roots of the fourth empirical eigenfunction were used as collocation points, thereby forcing the residual to be orthogonal, and therefore zero, at these points. Additional collocation points were added at $r = 0$ and $r = 1$ to satisfy the boundary conditions. Consequently, the dimension of the constructed low-order model was five. The ability of the fifth-order model to reproduce the solutions of the full-order model was tested in (Baker and Christofides, 1998) and was found to be excellent. This fifth-order model was used to synthesize a nonlinear multivariable output feedback controller using the controller synthesis formula of theorem 1 in (Baker and Christofides, 1998). The controller uses measurements of the wafer temperature at five locations across the wafer and adjusts the powers of the four top lamps (see Figure 1 for a schematic of the control configuration). We performed two sets of simulation runs to evaluate

the robustness properties of the nonlinear controller in the presence of significant model uncertainty and disturbances and compare them with the ones of a PI control scheme (which consists of four PI controllers; the tuning parameters were computed through extensive trial and error to obtain the best possible response). The values of the process parameters used in the simulations are given in (Baker and Christofides, 1998). In the first set of simulation runs, we consider a 40 *sec* cycle for the RTCVD process with initial conditions $T = 1$, $T_c = 1$, $S = 0$, $X_{SiH_4} = 0.1$ and $X_{H_2} = 0$. A 20 K decrease in the ambient temperature at $t = 15$ *sec* and a 20% reduction in the power of the side lamp bank B at $t = 30$ *sec* are considered as unmeasured disturbances. Figure 2 shows the spatiotemporal evolution of the wafer temperature under nonlinear control, while Figure 3 shows the thickness of the deposition at $t = 40.8$ *sec* under nonlinear (solid line) and PI (dashed line) control. It is clear that the nonlinear controller achieves uniform deposition of the thin film on the wafer (less than 1% nonuniformity) and outperforms the PI control scheme (more than 8% nonuniformity). In the second set of simulation runs, we consider a 40 *sec* cycle for the RTCVD process with initial conditions $T = 1$, $T_c = 1$, $S = 0$, $X_{SiH_4} = 0.1$ and $X_{H_2} = 0$. In this case, a 50% error in the emissivity of the wafer was introduced at $t = 15$ *sec*. Figure 4 shows the spatiotemporal evolution of the wafer temperature under nonlinear control, while Figure 5 shows the thickness of the deposition at $t = 40.8$ *sec* under nonlinear (solid line) and PI (dashed line) control. Again, the nonlinear controller achieves almost uniform deposition of the thin film on the wafer (less than 4% nonuniformity), while the PI control scheme leads to a significantly nonuniform response (more than 10% variation in final film thickness).

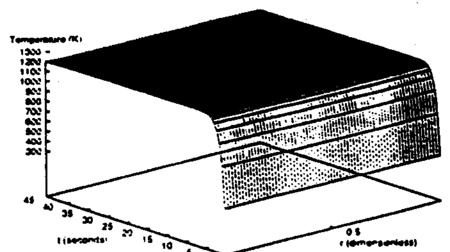

Fig. 2. Spatiotemporal wafer temperature profile under nonlinear control in the presence of disturbances in the ambient temperature and lamb bank B.

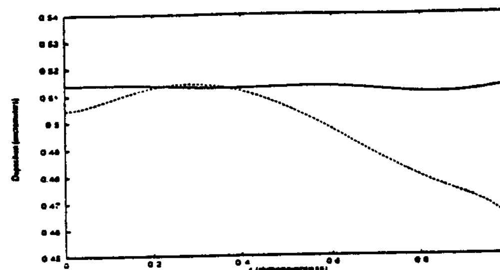

Fig. 3. Final film thickness in the presence of external disturbances under nonlinear control (solid line) and PI control (dashed line).

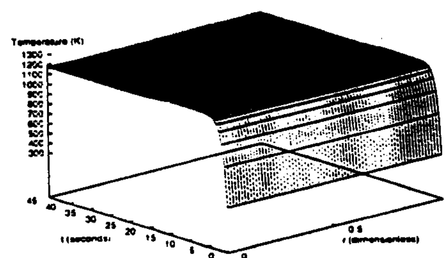

Fig. 4. Spatiotemporal wafer temperature profile under nonlinear control in the presence of parametric model uncertainty under nonlinear control.

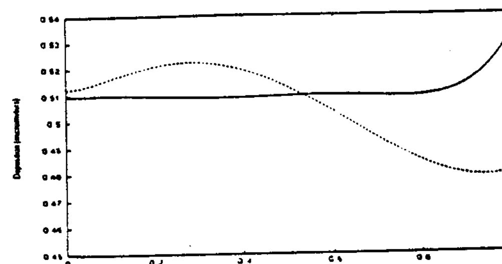

Fig. 5. Final film thickness in the presence of parametric model uncertainty under nonlinear (solid line) and PI control (dashed line).

4. REFERENCES

Aling, H., S. Benerjee, A. K. Bangia, V. Cole, J. Ebert, A. Emani-Naeini, K. F. Jensen, I. G. Kevrekidis and S. Shvartsman (1997). In: *Proc. of Amer. Contr. Conf.* Albuquerque, NM. pp. 2233–2238.

Baker, J. and P. D. Christofides (1998). *Inter. J. Contr.* submitted.

Breedijk, T., T. F. Edgar and I. Trachtenberg (1993). In: *Proc. of Amer. Contr. Conf.* San Francisco, CA. pp. 2980–2984.

Butler, S. W. and T. F. Edgar (1997). *AIChE Symposium Series* **93**, 133–144.

Kiether, W. J., M. J. Fordham, S. Yu, A. J. S. Neto, K. A. Conrad, J. R. Hauser, F. Y. Sorrell and J. J. Wortman (1994). In: *Proc. of 2nd Int. RTP Conf.* pp. 96–101.

Schaper, C. D. (1993). In: *Proc. of Amer. Contr. Conf.* San Francisco, CA. pp. 2985–2989.

Stuber, J. D., T. F. Edgar and T. Breedijk (1995). In: *Proc. of the Electrochem. Soc.* Reno, NV. pp. 113–147, (Vol. 4).

Theodoropoulou, A., E. Zafiriou and R. A. Adomaitis (1998*a*). In: *Proc. of DYCOPS-5.* pp. 29–34.

Theodoropoulou, A., R. A. Adomaitis and E. Zafiriou (1998*b*). *IEEE Trans. Sem. Manuf.* **11**, 85–98.